

Novel effects of localization due to ‘intrinsic disorder’ in the ‘two-fluid’ model for manganites

Prabuddha Sanyal^{1,2}, V.B. Shenoy², H. R. Krishnamurthy^{2,3}, and T. V. Ramakrishnan^{2,3,4}

¹ *School of Physics, Hyderabad Central University, Hyderabad- 500046*

² *Centre for Condensed Matter Theory (CCMT), Department of Physics, Indian Institute of Science, Bangalore 560012, India.*

³ *Jawaharlal Nehru Centre for Advanced Scientific Research, Bangalore 560064, India. and*

⁴ *Department of Physics, Banaras Hindu University, Varanasi 221005, India.*

We discuss the effects of a novel polaronic disorder in the recently proposed two-fluid model for manganites. Using effective field theory as well as direct numerical simulations, we show that this disorder can have dramatic effects in terms of the transition from ferromagnetic insulator to ferromagnetic metal upon hole-doping, including an Anderson localized regime where variable range hopping may be observed.

I. INTRODUCTION

Doped rare-earth manganites $A_{1-x}AE_xBO_3$ (A=Rare-Earth, AE=Alkaline Earth, B=Mn) are transition metal oxides where there is an intricate interplay of charge, orbital, spin and phonon degrees of freedom. No less important, however, is the role of disorder, which has dramatic effects upon the charge ordering, magnetic transition, etc¹. While many different types of disorder has been discussed in the context of manganites (eg. A-site disorder, B-site disorder etc.)²⁻⁴, in this paper we will introduce a novel kind of disorder apparently present in manganites but not widely talked about, and demonstrate its effects using the two-fluid (ℓ - b) model Hamiltonian⁵ which was proposed earlier for manganites.

The basic physics of manganites involve a coexistence of fast moving band electrons, and self-trapped JT polarons, interacting by Coulomb interaction, and strongly coupled to a background of core spins. The ‘ ℓ - b ’ model is an effective low energy Hamiltonian which implicitly captures the crucial effects of these interactions and the quantum dynamics of the JT phonons. It invokes two types of e_g electrons, one *polaronic* and *localized* (ℓ), and the other *band-like* and *mobile* (b), and is given by,

$$\begin{aligned}
 H_{\ell b} = & (-E_{JT} - \mu) \sum_{i,\sigma} n_{\ell i \sigma} - \mu \sum_{i,\sigma} n_{b i \sigma} \\
 & + U_{dd} \sum_{i,\sigma} n_{\ell i \sigma} n_{b i \sigma} - t \sum_{\langle ij \rangle, \sigma} (b_{i,\sigma}^\dagger b_{j,\sigma} + H.C.) \\
 & - J_H \sum_i (\vec{\sigma}_{\ell i} + \vec{\sigma}_{b i}) \cdot \vec{S}_i - J_F \sum_{\langle ij \rangle} \vec{S}_i \cdot \vec{S}_j \quad (1)
 \end{aligned}$$

The *polaronically trapped* ‘ ℓ ’ species has site energy $-E_{JT}$ (~ 0.5 eV), and an exponentially reduced hopping (~ 1 meV) which has been neglected, while the *non-polaronic* ‘ b ’ species (site energy 0) has undiminished hopping $t \sim 0.2$ eV. U_{dd} (~ 5 eV) is the effective on-site Coulomb repulsion between the ‘ ℓ ’ and

‘ b ’ species and J_H the aforementioned Hund’s coupling. J_F is a novel ferromagnetic *virtual double-exchange* coupling (~ 10 meV) between the core spins, which arises from *virtual, fast (adiabatic)* hopping processes of the ‘ ℓ ’ electrons to neighboring sites and back, leaving the local lattice distortion unrelaxed⁵. The chemical potential, μ , imposes the doping determined filling constraint: $\sum_{\sigma} (\langle n_{\ell \sigma} \rangle + \langle n_{b \sigma} \rangle) = (1 - x)$. At T=0, in the fully polarized ferromagnetic phase, it reduces to a form very similar to the Falicov-Kimball model⁶.

While disorder is commonly grouped into ‘annealed’ and ‘quenched’, we make a further distinction in the context of this $\ell - b$ model for manganites, namely: *intrinsic* and *extrinsic*. We note that from the basic premises of the $\ell - b$ Hamiltonian, the ℓ electrons are polaronically trapped at specific lattice sites, and have no quantum dynamics. They however, equilibrate according to classical statistical mechanics. The mobile b electrons hop in the background provided by these static ℓ polarons. Hence, the ℓ species represents an annealed disordered background to the mobile b species. We refer to this disorder as ‘intrinsic’, since it is ‘self-generated’ by the system under appropriate conditions. On the other hand, disorder due to doping at the A-site by alkaline earth atoms, or doping at the B-site by Aluminium, Chromium etc., is referred to as ‘extrinsic’. Thus, the b electrons face two kinds of disorder of the compositional type: namely *intrinsic, annealed* disorder due to the ℓ polarons⁷, and *extrinsic, quenched* disorder due to foreign dopant atoms. The effects of quenched disorder of the extrinsic type has already been considered in some detail in the literature, both at the abstract level^{8,9}, and in the specific context of manganites^{10,11}. In this paper we discuss the effects of this novel, intrinsic disorder in the context of the $\ell - b$ Hamiltonian for manganites.

The $\ell - b$ model has been studied using Dynamical Mean Field Theory (DMFT) in Ref⁵, which is exact in the limit of large dimensions. Due to the specific symmetries of the $\ell - b$ model, discussed in Ref⁵, it becomes exactly solvable in this limit, enabling a complete study of the phase diagram. However, DMFT, like its counterpart CPA (Coherent Potential Approximation), does

not include effects of Anderson localization which is a crucial effect of disorder at low temperatures, and which we want to focus on in this paper. The reason for this is discussed in more detail below. Hence, in this paper, we study the ℓ - b model using an approach pioneered by Vollhardt and Economou *et al* which can take us beyond the DMFT approximation. We also compare our results with studies of Inverse Participation Ratio (IPR) done using a direct numerical simulation.

II. DMFT OF L-B MODEL: SUMMARY

In the ℓ - b Hamiltonian, the mobile b electrons move in an annealed disordered background of site-trapped ℓ polarons. The DMFT approximation can be used to study the electronic and transport properties of this Hamiltonian. We first solve the DMFT exactly using semicircular DOS, and in the limit $U_{dd} \rightarrow \infty$ ⁵, in the fully spin-polarised ferromagnetic phase at $T=0$ ¹². The DMFT approximation reduces the complicated many-site problem given by Eqn 1 into an effective single-site problem, represented by the action:

$$\mathcal{A}_{DMFT}(n_\ell) = \sum_n [(\mathcal{G}_{bath}^{-1}(i\omega_n, \Omega_z) - U_{dd}n_\ell)\bar{b}_n b_n] - (E_{JT} - \mu)n_\ell \quad (2)$$

where n_ℓ is the fractional occupancy of ℓ -electrons at the DMFT site, and $\mathcal{G}(\omega)$ is the Weiss or bath Green's function. Solving this single site 'impurity' problem, we obtain the full impurity Green's function $G(\omega)$. Since this action is similar to that for the Falicov Kimball model⁶, hence it can be solved exactly. We can also obtain the exact self-energy for the b -electrons using the Dyson's equation:

$$\Sigma(\omega) = \mathcal{G}^{-1}(\omega) - G^{-1}(\omega) \quad (3)$$

This expression is given by:

$$\Sigma(\omega) = \left(1 - \frac{1}{W_0}\right) \mathcal{G}^{-1}(\omega) \quad (4)$$

where

$$\mathcal{G}(\omega) = \frac{2}{\omega + \sqrt{\omega^2 - W_0 D^2}} \quad (5)$$

and W_0 is the probability of there being no ℓ -polaron on the impurity site of the DMFT, to be determined self-consistently. For low dopings, $W_0 \approx x$. D is the half-bandwidth of the bare semicircular DOS.

The optical conductivity of a thermodynamic system can be obtained within linear response, using the Kubo formula:

$$\mathcal{R}\bar{\sigma}(\omega^+, q \rightarrow 0) = -\frac{1}{\omega d} \sum_{\alpha=1}^d \mathcal{I}\Pi_{\alpha\alpha}(\omega^+, q \rightarrow 0) \quad (6)$$

where $\Pi_{\alpha\beta}(\omega, q)$ is the well-known current-current correlation function. In the DMFT limit of large dimensions, only the elementary particle-hole Drude bubble for this correlation function survives, while all higher terms involving the irreducible vertex become negligible¹³. The contribution to the optical conductivity for a hypercubic lattice then becomes¹³:

$$\sigma(i\omega_n) = \frac{1}{\omega\beta} \sum_{k\nu_n\sigma} \frac{1}{d} \sum_{l=1}^d 4\sin^2(k_l) G(\vec{k}, i\nu_n) G(\vec{k}, i\nu_n + i\omega_n) \quad (7)$$

III. BEYOND DMFT: SELF-CONSISTENT THEORY OF LOCALIZATION

The DMFT approximation does not capture the physics of *Anderson Localization*, which may well be important for the low temperature transport behaviour of manganites having both intrinsic and extrinsic disorder. In particular, the Metal Insulator Transition (MIT) as a function of doping at low temperature is expected to be strongly influenced by localization physics. To investigate this aspect, we go beyond DMFT and study the mobility edge behaviour as a function of doping using the *Self-consistent Theory of Localization* (STS) developed by Vollhardt *et. al.*¹⁴. Economou *et. al.* had proposed a particularly simple, and practically useful prescription for finding the mobility edge by mapping the STS equations formally to equations for bound state formation in a potential well¹⁵. We use Economou's approach in this paper, which we refer to hereafter as *Potential Well Analogy* (PWA). We first find the single particle Green's function for the b -electrons, as well as the self-energy, using the DMFT approximation at zero temperature. The dc conductivity of the system is also found within the DMFT approach. Then we plug these quantities into the PWA equations to obtain the mobility edge at any particular doping.

In order to incorporate localization physics, one has to add correction terms to the Drude conductivity, obtained from 'maximally crossed' diagrams in the theory of weak localization¹⁶:

$$\sigma(\omega) \approx \sigma_0 - \frac{2e^2}{\pi\hbar(2\pi)^d} \int_{1/l_{in}}^{1/l_{el}} \frac{d\vec{k}}{k^2 - \frac{i\omega}{D_0}} \quad (8)$$

where σ_0 is the Drude conductivity, l_{el} is the elastic mean free path, while l_{in} is the inelastic mean free path. Using the Einstein relation between conductivity and diffusivity,

$$\sigma = 2e^2 \rho D_0 \quad (9)$$

one can rewrite eq 8 purely in terms of diffusivities. Now, the theory was made self-consistent by Vollhardt and Wolfe¹⁴ by replacing D_0 by the full $D(\omega)$ on the denominator of the integrand.

$$D(\omega) = D_0 - \frac{1}{\rho\pi\hbar(2\pi)^d} \int_{1/l_{in}}^{1/l_{el}} \frac{d\vec{k}}{k^2 - \frac{i\omega}{D(\omega)}} \quad (10)$$

The localization length λ was found by identifying $\frac{-i\omega}{D(\omega)} \rightarrow \frac{1}{\lambda^2}$ in the insulating regime.

Economou and Soukoulis¹⁵ pointed out that this equation has the same formal structure as the equation which determines the decay length of a bound state in a potential well.

$$\frac{1}{\Omega|V_0|} = \frac{2m^*}{(2\pi)^d\hbar^2} \int \frac{d^d k}{k^2 + k_b^2} \quad (11)$$

where Ω is the volume of the primitive unit cell, k_b is the inverse decay length of the bound state, while $|V_0|$ is the well depth, and m^* is the effective mass near the band bottom.

For the case of tight binding on a hypercubic lattice, one particular site has the well potential V_0 . Since the integral is over the Brillouin zone, one establishes a connection between the lattice constant a and the mean free path l_{el} , neglecting $1/l_{in}$ at low T . Now, knowing the minimum depth of the potential well necessary for the appearance of a bound state^{17,18}, one can estimate the mobility edge.

The mean free path $l(E)$ is found as usual:

$$l(E) = v(E)\tau(E) \quad (12)$$

$$= \frac{v_0(E - \mathcal{R}\Sigma(E))\hbar}{2I\Sigma(E)} \quad (13)$$

where $v_0(E)$ is defined as the average speed of Bloch waves over the surface of constant energy E .

The Drude conductivity $\sigma_0(E)$ can be found either in its full glory from Eq 7 or using the weak scattering approximation:

$$\sigma_0(E) \approx \frac{2e^2}{(2\pi)^d d\hbar} S_0(E - \mathcal{R}\Sigma(E))l(E) \quad (14)$$

where $S_0(E)$ is the area of the surface of constant energy.

IV. RESULTS

As discussed in detail in⁵, the $\ell - b$ model shows a transition from Ferromagnetic Insulator to Ferromagnetic metal, as the doping is increased, just as observed in real manganites. This is because of depletion in the number of trapped Jahn-Teller polarons, and corresponding decrease in scattering and increase in paths available for hopping, upon hole-doping. Within DMFT, for $U \rightarrow \infty$, the critical doping for this Insulator-Metal transition (IMT) can be obtained analytically as

$$x_c^{DMFT} = \left(\frac{E_{JT}}{D} \right)^2 \quad (15)$$

which corresponds to the doping where the bottom edge of the b -band hits the sharp level at energy E_{JT} corresponding to Jahn-Teller trapped ℓ -polarons. Since for $U \rightarrow \infty$ the DMFT b -electron DOS is proportional to the imaginary part of the bath Green's function mentioned above, they have the same bandwidth $\tilde{D} = \sqrt{W_0}D$, as is evident from Eq 5. Hence, when the b -band bottom hits the polaronic level, $\tilde{D} = E_{JT}$, giving the relation Eq 15 above. For $x < x_c$, the entire $(1-x)$ fraction of electrons were polaronically trapped in the local E_{JT} level, giving a polaronic insulator. For $x > x_c$, the b -band states are available for the electrons to delocalize, which according to DMFT, should immediately lead to a metallic state. We would like to improve upon this picture in this paper by bringing in the effect of Anderson localization.

We calculate the relaxation time τ , mean free path l and transport DOS $v(E)S(E)$ for a cubic lattice and a single-orbital, tightbinding band. The DMFT parameters are chosen so that the bottom edge of the b -band hits the sharp ℓ -level at a doping (x_c^{DMFT}) of about 0.25. On account of the exact analytic relation mentioned above, this is accomplished by choosing, *eg.*, E_{JT} to be -3 in units of hopping. This is because, for a cubic lattice, the half bandwidth is $6t$, which we identify with the half-bandwidth D of the semicircular DOS mentioned above. Thus $D = 6$ in units of hopping t . The mobility edges are calculated both using the full conductivity, and the weak-scattering assumption as in Eq 14.

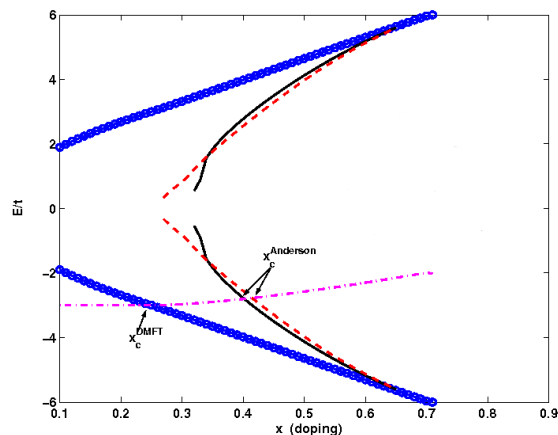


FIG. 1: (colour online) mobility edge trajectory vs doping. Circles (blue): band edges. Dash-dot line (red): Fermi energy. Solid Lines (black): Mobility edges using actual DMFT conductivity. Dashed lines (red): Mobility edges using weak scattering approximation. Parameters: $E_{JT}/t = -3$, $D/t = 6$

The mobility edge trajectories obtained by both methods are plotted as a function of the doping in Fig 1. One finds that for either method, there are two mobility edges occurring symmetrically about the centre of the band, between which lie the extended states. States lying between any one mobility edge and the band edge on the same side are localized, since it is the band tails which get localized first. For low doping values below x_c^{DMFT} , all states in the band are localized, and both the mobility edges are

coincident at the band centre. As the doping increases, both the mobility edges proceed outwards from the band centre. Simultaneously, the bandwidth also increases (roughly as $\sqrt{x}D$ for low doping values), due to reduced scattering from polarons. The rate at which the mobility edges move apart in energy with increasing doping is greater than the rate at which the bandwidth increases, so that ultimately, the mobility edges meet the corresponding band edges at a large enough doping (≈ 0.6 for this parameter set). This means that beyond this doping value all states in the band are extended. This makes sense, because nearabout this large doping, there are no more ℓ -polarons left ($W_1 = 0$). This means that the b -electrons do not encounter any scattering, and the bandwidth is at its maximum. It is to be noticed that the mobility edge trajectories calculated by the two methods differ significantly only for small doping, while they coincide for large doping. This is to be expected, since for smaller doping values, there are a substantial number of polaron scatterers, so that the weak-scattering assumption is not justified.

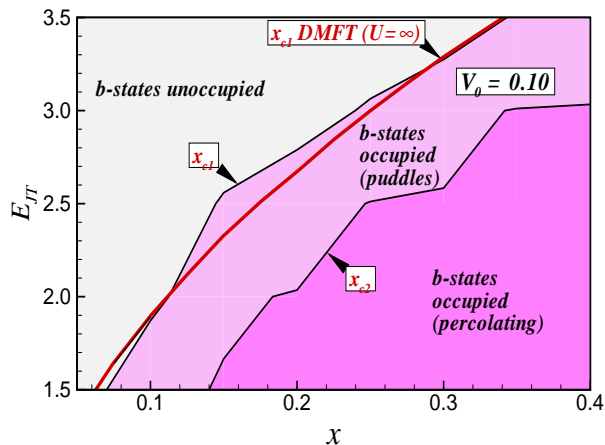


FIG. 2: E_{JT} vs x showing various phase boundaries, along with the DMFT parabola for comparison.

We have also plotted the self-consistently determined value of chemical potential from the DMFT, on the same graph. It is found that even though the b -band states begin to become occupied for $x > x_c^{DMFT}$, but for a range of x thereafter, the occupied states are localized. The chemical potential proceeds towards the band centre, and meets the lower mobility edge at a doping $x_c^{Anderson}$ of the order of 0.4. Hence, for intermediate values of doping $x_c^{DMFT} < x < x_c^{Anderson}$, the system is an *Anderson Insulator*, although DMFT predicts that it should be metallic.

We now compare this result, obtained using effective field theories, with a more realistic, real space, finite-size simulation of the $\ell - b$ model (in the fully polarised ferromagnetic phase at $T=0$), done by V. Shenoy *et.al.*¹⁹. Details of this simulation will be found in Ref²⁰. In this simulation, in addition to the Hamiltonian described before, there is a long range Coulomb interaction between charges. This long-range Coulomb interaction (treated

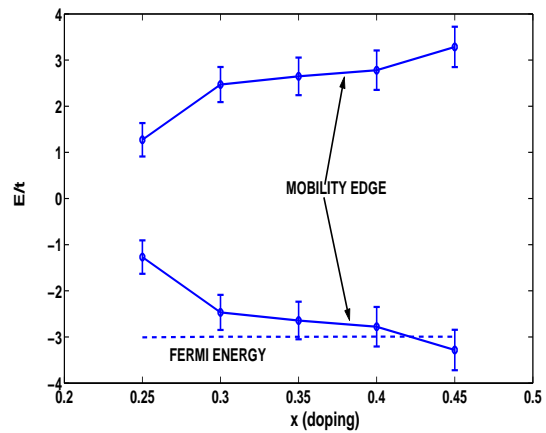


FIG. 3: mobility edge trajectory vs doping from real space numerical simulation

using Hartree-Fock approximation) prevents phase separation, and bring about a somewhat ‘homogeneous’ mixture of ℓ and b , as is assumed in DMFT. The presence of this long range Coulomb interaction, along with the compensating negative charge for the dopant atoms, gives an additional source of disorder that was not included in the effective medium calculations. However, this disorder is correlated, as compared to the uncorrelated disorder due to the ℓ -polarons. One finds that this additional correlated disorder seems to make very little difference from DMFT results with regard to the ‘critical’ doping required for electrons to start occupying band states. This is observed in Fig 2, where the phase boundary for b -state occupancy nearly coincides with the DMFT parabola given by Eq 15.

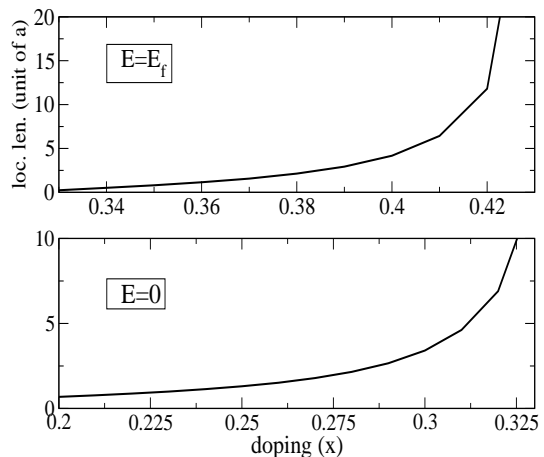


FIG. 4: Doping variation of localization length evaluated at the Fermi energy (top) and at the center of the band (bottom)

We refer to this ‘critical’ value of doping as $x_c^{occupancy}$. One finds that this $x_c^{occupancy} \approx x_c^{DMFT}$. However, in

this real space simulation, even after b -band states begin to get occupied, the hole clumps within which b -electrons are allowed to hop (for on-site $U_{dd} \rightarrow \infty$) may not be percolating. We call the ‘critical’ doping for this percolation threshold as $x_c^{percolation}$, and this is higher than $x_c^{occupancy}$. Moreover, even within these percolating clumps, some of the b -electron states may be Anderson localized. To check the character of these band states, we find the *Inverse Participation Ratio* (IPR), defined as follows:

$$IPR = \frac{\sum_i^N |a_i|^4}{(\sum_i^N |a_i|^2)^2} \quad (16)$$

where a_i is the amplitude of the state at the i -th site. For an extended state, a_i goes as $e^{i\vec{k}\cdot\vec{R}_i}$, so that $|a_i| = 1$, and $IPR \rightarrow \frac{1}{N} \rightarrow 0$ for large N . But for a state localized at the j -th site, $a_i = \delta_{ij}$, and $IPR \rightarrow 1$. Hence, IPR gives a good criterion for distinguishing extended states from localized ones.

Since different realizations of the compensating dopant charge distribution give different set of states, one gets a distribution of IPR within each small energy range inside the band. Hence, we discretize the band into energy intervals, and find the probability distribution for IPR within each such interval, by plotting histograms and corresponding frequency polygons, as discussed in detail in Ref²¹. One finds from Fig 3 that the mobility edge trajectories once again proceed away from the band centre, and towards the edges as doping increases. Moreover, the chemical potential, determined from the band-filling in the same simulation, lies between the lower band edge and the lower mobility edge for small doping. Hence, this simulation also predicts the existence of an Anderson Insulator phase for a certain region of doping. Moreover, the value of $x_c^{Anderson} \approx 0.4$ obtained from Fig 3, also agrees closely with the effective field theory calculations described before. Thus, for $E_{JT} = 3$, the $x_c^{occupancy} \approx 0.25$, $x_c^{percolation} \approx 0.33$, while $x_c^{Anderson} \approx 0.4$ ²².

We have also calculated the localization length λ as a function of doping using the PAW formalism. It turns out to be surprisingly small near x_c^{DMFT} : namely of the order of a lattice spacing, even less for lower doping values.

As one approaches $x_c^{Anderson}$, λ at Fermi energy diverges, as expected. λ for states at the center of the band diverge for lesser x , since the mobility edge trajectories converge to the center at around $x = 0.3$. Variable range hopping is therefore expected to be observed in the Anderson Insulator regime from x_c^{DMFT} to $x_c^{Anderson}$. The resistivity is therefore expected to go as^{23,24} $exp(T_0/T)^{1/4}$, where the temperature parameter T_0 is given by $T_0 = \frac{18\alpha^3}{k_B N(E_F)}$, α being the inverse localization length. From our calculation of localization length, we estimate this parameter to lie between $10^7 - 10^8 K$ in this doping regime.

In conclusion, we have extended the DMFT calculations for the IMT within the two-fluid model⁵ for manganites to incorporate localization effects. We find the existence of a prominent Anderson Insulator phase in addition to the polaronic, percolative insulator phases seen before. Such an Anderson Insulator phase may well explain the observations of variable range hopping (VRH)⁹ in manganites reported by experimentalists²⁵⁻³⁰. The exceptionally small λ in the Anderson Insulating regime should translate to a large value for the temperature parameter for the VRH, as suggested by these studies. In the real space simulations by Shenoy *et.al.*²⁰, there exists a Coulomb glass phase with a soft Coulomb gap at low doping values prior to the occupancy of the b -band states. This is due to the site-trapped ℓ polarons, which also interact with each other by Coulomb interaction. This should give rise to a Shklovskii-Efros (SE-VRH) $T^{1/2}$ transport²⁴, which in this scenario will crossover into the Mott-VRH $T^{1/4}$ regime as the doping is increased, and the b -band states begin to get occupied, before the final Insulator-Metal transition. Interestingly, both the SE-VRH and Mott-VRH regimes have been noticed and reported in the experimental literature^{31,32}, and there exists considerable debate between which one is more applicable to manganites. This is partly because of the technical difficulty associated with distinguishing between various power-laws in the exponent by fitting the resistivity data within a limited range of temperature³². Our calculation, together with the earlier ones by Shenoy *et.al.*, on the other hand, postulate the existence of *both* the SE-VRH and Mott-VRH regimes at different values of doping within the phase diagram for manganites.

¹ For reviews, see *Colossal Magnetoresistive Oxides*, ed. by Y. Tokura (Gordon and Breach, Amsterdam, 2000).

² Y. Sawaki, K. Takenaka, A. Osuka, R. Shiozaki, S. Sugai, Phys. Rev. B, **61**, 11588.

³ K. Takenaka, S. Okuyama, R. Shiozaki, T. Fujita, S. Sugai, J. Appl. Phys., **91**, 2994 (2002).

⁴ N. Rama *et. al.*, Phys. Rev. B, **70**, 224424 (2004).

⁵ T.V. Ramakrishnan, H.R. Krishnamurthy, S.R. Hassan and G.V. Pai, Phys. Rev. Lett., **92**, 157203 (2004); G.V. Pai, S.R. Hassan, H.R. Krishnamurthy and T.V. Ramakrishnan, EuroPhys. Lett. **64**, 696 (2003); G. Venketeswara

Pai, Ph.D. Thesis, Indian Institute of Science (2002); S.R. Hassan, Ph.D. Thesis, Indian Institute of Science (2003).

⁶ J. K. Freericks and V. Zlatic, Rev. Mod. Phys. **75**, 1333 (2003).

⁷ *50 years of Anderson localization*, ed. by E. Abrahams, (World Scientific Review Volume, 2010).

⁸ B. Kramer and A. Mackinnon, Rep. Prog. Phys., **56**, 1469 (1993).

⁹ P.A. Lee and T.V. Ramakrishnan, Rev. Mod. Phys., **57**, 287 (1985).

¹⁰ S. Kumar and P. Majumdar, Phys. Rev. Lett., **96**, 016602

- (2006).
- ¹¹ S. Kumar and A.P. Kamph, Phys. Rev. B, **77**, 134442 (2008).
- ¹² The self-energy, critical doping etc. for the DMFT done explicitly considering the DOS for a cubic lattice, and with finite but large U , does not vary appreciably from that for semicircular DOS, and $U \rightarrow \infty^5$. The latter, however, gives the advantage of obtaining exact analytical expressions. We have repeated the mobility edge calculation with the DMFT done numerically using cubic DOS, and the results turn out to be similar in all aspects.
- ¹³ A. Georges, G. Kotliar, W. Krauth and M.J. Rozenberg, Rev. Mod. Phys., **68**, 13 (1996).
- ¹⁴ D. Vollhardt and P. Wolfe, Phys. Rev. B, **22**, 4666 (1980); D. Vollhardt and P. Wolfe, Phys. Rev. Lett., **45**, 482 (1980).
- ¹⁵ E. N. Economou and C.M. Soukoulis, Phys. Rev. B, **28**, 1093 (1983).
- ¹⁶ G. Bergmann, Physics Reports, **107**, 1 (1984).
- ¹⁷ E. N. Economou, *Green's functions in Quantum Physics* (Springer, Heidelberg, 1979).
- ¹⁸ E. N. Economou, C.M. Soukoulis and A.D. Zdtetis, Phys. Rev. B, **30**, 1686 (1984).
- ¹⁹ V.B. Shenoy, T. Gupta, H.R. Krishnamurthy and T.V. Ramakrishnan, Phys. Rev. Lett., **98**, 097201 (2007).
- ²⁰ V.B. Shenoy, T. Gupta, H.R. Krishnamurthy and T.V. Ramakrishnan, cond-mat/0606660, 2006.
- ²¹ Prabuddha Sanyal, Ph.D. Thesis, Indian Institute of Science (2007).
- ²² It is to be noted that these values for the critical dopings themselves are not to be considered sacrosanctly, but only as exhibiting the trend that we wish to highlight. In order to match with real manganites, the parameters like bandwidth, E_{JT} etc. has to be chosen appropriately so that the various x_c have more realistic values.
- ²³ N.F. Mott, *Metal Insulator Transitions*, (Taylor & Francis, 1990).
- ²⁴ B.I. Shklovskii and A.L. Efros, Electronic properties of doped semiconductors, (Springer-Verlag, Berlin, 1984).
- ²⁵ Mixed Valence Manganites, *Advances in Physics*, **48**, 167 (1999)
- ²⁶ J.M.D. Coey, M. Viret, L. Ranno and K. Ounadjela, Phys. Rev. Lett., **75**, 3910 (1995).
- ²⁷ Viret M, Ranno L and Coey J.M.D., Phys. Rev. B, **55**, 8067.
- ²⁸ Viret M, Ranno L and Coey J.M.D., J. Appl. Phys., **81**, 4964 (1997).
- ²⁹ H. Jain, A.K. Raychaudhuri, Y.M. Mukovskii and D. Shulyatev, App. Phys. Lett., **89**, 152116 (2006).
- ³⁰ Y. Sun, X. Xu and Y. Zhang, J. Phys. Condens. Mat., **12**, 10475 (2000).
- ³¹ A Biswas, S. Elizabeth, A.K. Raychaudhuri, H.L. Bhat, Phys. Rev. B, **59**, 5368, (1999).
- ³² R. Laiho, K.G. Lisunov, F. Lahderanta, V.N. Stamov and V.S. Zakhvalinskii, J. Phys.: Condens. Matter, **13**, 1233 (2001).